ENSO Modulates Mean Currents and Mesoscale Eddies in the Caribbean Sea

Minghai Huang[1], Xinfeng Liang[1], Yang Yang[2], and YANG ZHANG[3]

[1]University of Delaware
[2]Nanjing University of Information Science and Technology
[3]School of Marine Science and Policy, College of Earth, Ocean, and Environment, University of Delaware

April 16, 2023

Abstract

Although ENSO and its global impacts through teleconnection have been known for decades, if and how the mean currents and mesoscale eddies in the Caribbean Sea are linked to ENSO remains an open question. Here, by analyzing satellite observations and an ocean reanalysis product, we found a close connection between mean currents, eddies in the Caribbean Sea and ENSO on interannual timescales. Strong El Niño events result in enhanced north-south sea surface height (SSH) differences and consequently stronger mean currents in the Caribbean Sea, and the opposite happens during La Niña events. The eddy kinetic energy (EKE) responses to ENSO via eddy-mean flow interaction, primarily through baroclinic instability, which releases the available potential energy stored in the mean currents to mesoscale eddies. Our results suggest some predictability of the mean currents and eddies in the Caribbean Sea, particularly during strong El Niño and La Niña events.

Hosted file

960039_0_art_file_10866661_rsn8qj.docx available at https://authorea.com/users/554169/articles/633932-enso-modulates-mean-currents-and-mesoscale-eddies-in-the-caribbean-sea

Hosted file

960039_0_supp_10855888_rsfbyw.docx available at https://authorea.com/users/554169/articles/633932-enso-modulates-mean-currents-and-mesoscale-eddies-in-the-caribbean-sea

ENSO Modulates Mean Currents and Mesoscale Eddies in the Caribbean Sea

Minghai Huang[1*], Xinfeng Liang[1], Yang Yang[2], Yang Zhang[1]

[1]School of Marine Science and Policy, University of Delaware, Lewes, DE 19958

[2]State Key Laboratory of Marine Environmental Science, College of Ocean and Earth Sciences, Xiamen University, Xiamen, China.

Corresponding author: Minghai Huang (minghaih@udel.edu)

Key Points

- Interannual variations of mean currents and eddies in the Caribbean Sea are linked to ENSO
- ENSO-induced wind pattern changes modulate the north-south SSH differences and hence the mean currents in the Caribbean Sea
- Interannual variation of eddy kinetic energy in the Caribbean Sea is controlled by baroclinic instability

Abstract

Although ENSO and its global impacts through teleconnection have been known for decades, if and how the mean currents and mesoscale eddies in the Caribbean Sea are linked to ENSO remains an open question. Here, by analyzing satellite observations and an ocean reanalysis product, we found a close connection between mean currents, eddies in the Caribbean Sea and ENSO on interannual timescales. Strong El Niño events result in enhanced north-south sea surface height (SSH) differences and consequently stronger mean currents in the Caribbean Sea, and the opposite happens during La Niña events. The eddy kinetic energy (EKE) responses to ENSO via eddy-mean flow interaction, primarily through baroclinic instability, which releases the available potential energy stored in the mean currents to mesoscale eddies. Our results suggest some predictability of the mean currents and eddies in the Caribbean Sea, particularly during strong El Niño and La Niña events.

Plain Language Summary

We, in this study, explore the potential impacts of ENSO on the mean circulation and mesoscale eddies in the Caribbean Sea. We found ENSO-related synchronized changes in mean currents and eddies across the entire Caribbean Sea. The connection between the mean currents and ENSO is established through ENSO's impact on the north-south sea surface height (SSH) difference in the Caribbean Sea, which determines the strength of the geostrophic jet. During strong El Niño events, the easterly wind anomalies will increase the north-south SSH difference through Ekman transport, and consequently generate stronger mean currents. During strong La Niña events, the opposite happens. Through baroclinic instability, available potential energy stored in the mean currents will be transferred to eddies and results in ENSO-modified interannual variations of EKE. Our results suggest that interannual variations of mean currents and eddies in the Caribbean Sea might be predictable, particularly during strong El Niño and La Niña events.

1. Introduction

The Caribbean Sea is a critical region connecting the tropical Atlantic, the Gulf of Mexico, and the North Atlantic Ocean. The mean circulation in the Caribbean Sea is characterized by currents from the Lesser Antilles to the Yucatan Channel into the Gulf of Mexico (GoM, Gordon, 1967; Johns et al., 2002) and is a major pathway for transporting mass, heat, salt, and other tracers in the Atlantic Circulation System. Mesoscale eddies are also ubiquitous in the Caribbean Sea (Pratt & Maul, 2000; Jouanno et al., 2012; van der Boog et al., 2019a, 2019b; López-Álzate et al., 2022). These eddies advect cold filaments, modulate heat balance in the interior of the Caribbean Sea, and affect the temperature variability through the upwelling in the Cariaco Basin (Astor et al., 2003; Jouanno & Sheinbaum, 2013). They also transport nutrients, chlorophyll, *Sargassum*, larvae and pollutants, and hence impact the ecosystem (Andrade & Barton, 2005; Chérubin & Richardson, 2007; E. M. Johns et al., 2014; Andrade-Canto et al., 2022). In addition, some studies suggest that the eddies in the Caribbean Sea could impact the eddy-shedding of the Loop Current in the Gulf of Mexico (e.g., Murphy et al., 1999; Oey et al., 2004; Yang et al., 2020; Andrade-Canto et al., 2020; Huang et al., 2021; Laxenaire et al., 2023; Ntaganou et al., 2023).

Some aspects of the interannual variability of mean currents and eddies in the Caribbean Sea have been studied. For instance, previous studies indicate that interannual variations of the Caribbean Current is related to the north–south sea surface height (SSH) difference, which is driven by the changing wind pattern (Alvera-Azcárate et al., 2009). In addition, baroclinic and barotropic instabilities of the mean current can affect the Caribbean eddies (Carton & Chao, 1999; Andrade & Barton, 2000; Richardson, 2005; Jouanno et al., 2009, 2012). In the central Caribbean Sea (Colombia Basin), Jouanno et al. (2012) show that mean kinetic energy (MKE) and eddy kinetic energy (EKE) are related and exhibit a close relationship with wind stress. Moreover, a recent study using Self-Organizing Maps reveals interannual EKE variabilities in the Caribbean Sea, but no further investigation of the underlying mechanisms has been conducted (López-Álzate et al., 2022).

ENSO teleconnection and its impacts on remote regions have been known for decades (Alexander et al., 2002; Yeh et al., 2018). In the Caribbean Sea, previous studies show that ENSO can affect wind stress, temperature, rainfall pattern, net primary production, and chlorophyll (e.g., Enfield & Mayer, 1997; Malmgren et al., 1998; Giannini et al., 2001; Maldonado et al., 2016; Taylor et al., 2012; Chang and Oey, 2013; Muller-Karger et al., 2019; Sayol et al., 2022). Early studies based on tide gauges and altimetry also suggest that interannual variations of the sea level in the Caribbean Sea are correlated with ENSO (Alvera-Azcárate et al., 2009; Palanisamy et al., 2012). Some recent studies directly link the interannual anomalous wind pattern in the Caribbean region to ENSO (Dong et al., 2022; Sayol et al., 2022).

As mentioned above, ENSO can modulate various quantities in the Caribbean Sea. Now a few questions naturally arise: 1) Will the ENSO-induced winds and sea level variations result in changes in the geostrophic jet that is driven by the north–south SSH difference? 2) How do the mesoscale eddies in the Caribbean Sea respond to the variations of mean currents? In this study, we will try to answer these questions by analyzing altimetry observations and one oceanic reanalysis product. We will focus on possible roles of ENSO in modulating the MKE and EKE in the whole Caribbean Sea. The rest of the paper is organized as follows: Section 2 describes the data and methods used in this study. Section 3 presents the results of the interannual variations of MKE, EKE, their relationships with ENSO, and the underlying mechanisms. The results are summarized and discussed in Section 4.

2. Data and Methods

a. Data

Satellite altimetry products, including the sea level anomalies (SLA), absolute dynamic topography (ADT), and geostrophic currents, are used to characterize the surface eddy characteristics and validate the reanalysis product. They are distributed by the Copernicus Marine Environment Monitoring Service (CMEMS). The SLA is referenced to a 20-year (1993-2012) mean (Pujol et al., 2016). The altimetry data has $0.25^{\circ} \times 0.25^{\circ}$ horizontal resolution and daily temporal intervals. The altimetry data from 1993 to 2020 are used in this study.

A global ocean reanalysis product, Forecast Ocean Assimilation Model from Met Office (FOAM; Blockley et al., 2014), is used to describe and understand the interannual variability of mean currents and eddies. FOAM is distributed by the Copernicus Marine Environment Monitoring Service (CMEMS) Global Ocean Ensemble Reanalysis project. It is a homogeneous 3D gridded description of the physical state of the ocean constrained with satellite and in situ observations (Blockley et al., 2014). Its temporal range is from 1993 to 2020. It has $0.25^{o} \times 0.25^{o}$ horizontal resolution, 75 vertical levels and daily time intervals. The vertical resolution varies from a few meters near the sea surface to ~200 m near the bottom. FOAM reproduces the low-frequency mean and eddy variabilities in the Caribbean Sea reasonably well (shown later in Section 3). This product was also recently utilized in a similar study in the North Brazil region (Huang et al., 2023).

Monthly averaged surface 10 m wind from the European Centre for Medium-Range Weather Forecasts Reanalysis (Hersbach et al., 2020) is used to explore the possible forcing for the variations in mean currents and mesoscale eddies. The temporal range of the wind data is from 1993 to 2020. It has a $0.25^{o} \times 0.25^{o}$ horizontal resolution.

The daily sea surface temperature (SST) reprocessed product (Good et al., 2020) is used to investigate possible links between ENSO, mean currents and eddies. It has a $0.05^{o} \times 0.05^{o}$ horizontal resolution. Niño3.4, NAO (North Atlantic Oscillation) as well as AMO (Atlantic Multi-decadal Oscillation) indices are used to explore the relationships of various climate variabilities with mean currents and eddies in the Caribbean Sea. To be consistent with the other datasets, time ranges of SST and climate indices used in this study are between 1993 and 2020.

b. Analyses

The multiscale window transform (MWT) and the MWT-based localized multiscale energy analysis (Liang, 2016) are used to investigate the mean currents and eddy variabilities as well as the underlying dynamic mechanisms in the Caribbean Sea. This time-varying multiscale energetics framework is based on a new functional analysis apparatus, namely, MWT (Liang & Anderson, 2007). A brief description of this method is provided below and for more detailed information refer to Liang (2016).

The MWT-based multiscale ocean energetic equations for the multiscale KE (K^{ϖ}) and available potential energy (APE, A^{ϖ}) can be obtained as:

$$\frac{\partial K^{\varpi}}{\partial t} = \underbrace{-\nabla\cdot[\frac{1}{2}[\widehat{(\mathbf{vv}_h)}^{\sim\varpi}\cdot\hat{\mathbf{v}}_h^{\sim\varpi}]]}_{-\nabla\cdot\boldsymbol{Q}_k^{\varpi}} + \underbrace{\frac{1}{2}[\widehat{(\mathbf{vv}_h)}^{\sim\varpi}:\nabla\hat{\mathbf{v}}_h^{\sim\varpi} - \nabla\cdot\widehat{(\mathbf{vv}_h)}^{\sim\varpi}\cdot\mathbf{v}_h^{\sim\varpi}]}_{\Gamma_k^{\varpi}}$$

$$\underbrace{-\nabla\cdot(\frac{1}{\rho_0}\hat{\mathbf{v}}^{\sim\varpi}\hat{\mathrm{P}}^{\sim\varpi})}_{-\nabla\cdot\boldsymbol{Q}_P^{\varpi}} + \underbrace{(-\frac{g}{\rho_0}\hat{\rho}^{\sim\varpi}\hat{\mathrm{w}}^{\sim\varpi})}_{b^{\varpi}} + \mathrm{F}_K^{\varpi}, \qquad (1)$$

$$\frac{\partial A^{\varpi}}{\partial t} = \underbrace{-\nabla\cdot\left[\frac{1}{2}c\hat{\rho}^{\sim\varpi}\widehat{(\mathbf{v}\rho)}^{\sim\varpi}\right]}_{-\nabla\cdot\boldsymbol{Q}_A^{\varpi}} + \underbrace{\frac{c}{2}[\widehat{(\mathbf{v}\rho)}^{\sim\varpi}\cdot\nabla\hat{\rho}^{\sim\varpi} - \rho^{\sim\varpi}\nabla\cdot\widehat{(\mathbf{v}\rho)}^{\sim\varpi}]}_{\Gamma_A^{\varpi}}$$

$$\underbrace{+\frac{g}{\rho_0}\hat{\rho}^{\sim\varpi}\hat{\mathrm{w}}^{\sim\varpi}}_{-b^{\varpi}} + \underbrace{\frac{1}{2}\hat{\rho}^{\sim\varpi}\widehat{(\mathrm{w}\rho)}^{\sim\varpi}\frac{\partial c}{\partial z}}_{\mathrm{S}_A^{\varpi}} + \mathrm{F}_A^{\varpi}, \qquad (2)$$

where $\varpi = 0, 1$ stands for the mean current and eddy window, respectively. The definition of KE and APE on scale window ϖ are $K^{\varpi} = \frac{1}{2}\hat{\boldsymbol{v}}_h^{\sim\varpi}\cdot\hat{\boldsymbol{v}}_h^{\sim\varpi}$, $A^{\varpi} = \frac{1}{2}c\,(\hat{\rho}^{\sim\varpi})^2$. $\widehat{(\cdot)}^{\sim\varpi}$denotes MWT on window ϖ. $\boldsymbol{v}_h$ is the horizontal velocity, $c = g^2/\rho_0^2N^2$, N is the Brunt–Väisälä frequency. ρ_0 is the reference density (1025 kg m^{-3}). ρ is the density anomaly (with the mean vertical profile $\underline{\rho}(z)$ removed). Variabilities of KE (*K*) and APE (*A*) on the left side are controlled by the dynamics processes on the right side, where $-\nabla\cdot Q_k^{\varpi}$ and $-\nabla\cdot Q_A^{\varpi}$ are the advection of K^{ϖ} and A^{ϖ}, respectively. $-\nabla\cdot Q_P^{\varpi}$ is the pressure flux convergence. Γ_k^{ϖ} and Γ_A^{ϖ} are cross-scale transfers of KE and APE to window ϖ from other windows, standing for the redistribution of energy among different scales (Figure S1). $\Gamma_k^{0\to1}$and $\Gamma_A^{0\to1}$ are barotropic transfer (BT) and baroclinic transfer (BC), respectively. The b^{ϖ} terms are the buoyancy conversion between KE and APE. S_A^{ϖ} is the result from the vertical shear of c (a source/sink of A^{ϖ}). F_K^{ϖ} and F_A^{ϖ} are residual terms including contributions from dissipation, external forcing, and subgrid processes. Detailed expressions and meanings of the symbols are listed in Table S1.

To separate mean currents and eddies with the MWT approach, an eddy scale level or a cutoff period of eddies needs to be determined. Early numerical studies in the Caribbean Sea set the mesoscale window shorter than 120 or 125 days (Jouanno et al., 2012; van der Boog et al., 2019b). Recently, based on 27 years of satellite altimetry data, López-Álzate et al. (2022) identified that the average lifetime for all the eddies is 62 ± 37 days (mean ± standard deviation) and most eddies (~90%) have a lifetime shorter than 160 days in the Caribbean Sea. Based on previous studies, a period shorter than 160 days appears to be an appropriate choice for the cut-off period of the mesoscale window. We have also tested ~120 days as the scale level bound, and the results are quantitatively similar.

To further explore how ENSO modulates the mean currents and eddies, potential factors like wind, SST, SLA, and geostrophic currents in the Caribbean Sea are linearly regressed into the Niño3.4 index. Since we focused on the role of ENSO, monthly climatology and linear trends are removed and a 2-year lowpass filter is applied. We also tested 1- and 3-year lowpass filter, and the results are similar.

3. Results

MKE and EKE in the Caribbean Sea from the altimetry and FOAM are shown in Figure 1. We first examine to what extent the altimetry and FOAM results agree. Mean currents from the altimetry and FOAM, displayed as high MKE from the Lesser Antilles to the Yucatan Channel, have similar spatial distribution (Figure 1a, b). In the three basins (i.e., the Colombia Basin, the Venezuela Basin, and the Cayman Basin), similar interannual variabilities (Figure 1e-g) and significantly high correlations between altimetry and FOAM MKEs also appear. For the EKE (Figure 1i-k), although the FOAM values are smaller than those of the altimetry (similar to the MKE), their temporal evolutions agree reasonably well. The agreements of MKE/EKE from the altimetry and FOAM confirm that FOAM can be used to examine the interannual variations of mean currents and eddies in the Caribbean Sea, as well as the underlying mechanisms.

We then examine the evolutions of MKE and EKE in the three basins of the Caribbean Sea. We first look at the MKE (Figure 1e-g). Evident synchronized interannual variations of MKE among the three basins are presented in both altimetry and FOAM. More specifically, in all the three basins, high MKE appears in 1994-1995, 1997-1998, 2015-2016, 2019-2020, and low MKE appears in 1993-1994, 1999-2000, 2017-2018, and 2020-2021. The synchronized variations of MKE are also reflected in high correlations of MKE in different ocean basins, with 0.74 between the Colombia and Venezuela Basins, and 0.77 between the Colombia and Cayman Basins. For EKE, similar synchronized temporal variations revealed in MKE are also exhibited. The EKE correlation coefficients are 0.71 between the Colombia and Venezuela Basins, and 0.71 between the Colombia and Cayman Basins. In addition, higher MKE/EKE in 1997-1998, 2015-2016 (strong El Niño events), and lower MKE/EKE in 2020-2021 (one strong La Niña event) suggest an important role of ENSO on the interannual variations of the mean currents and eddies in the Caribbean Sea. This is further confirmed by significantly high correlations between Niño3.4 and MKE/EKE in the three basins (Table 1).

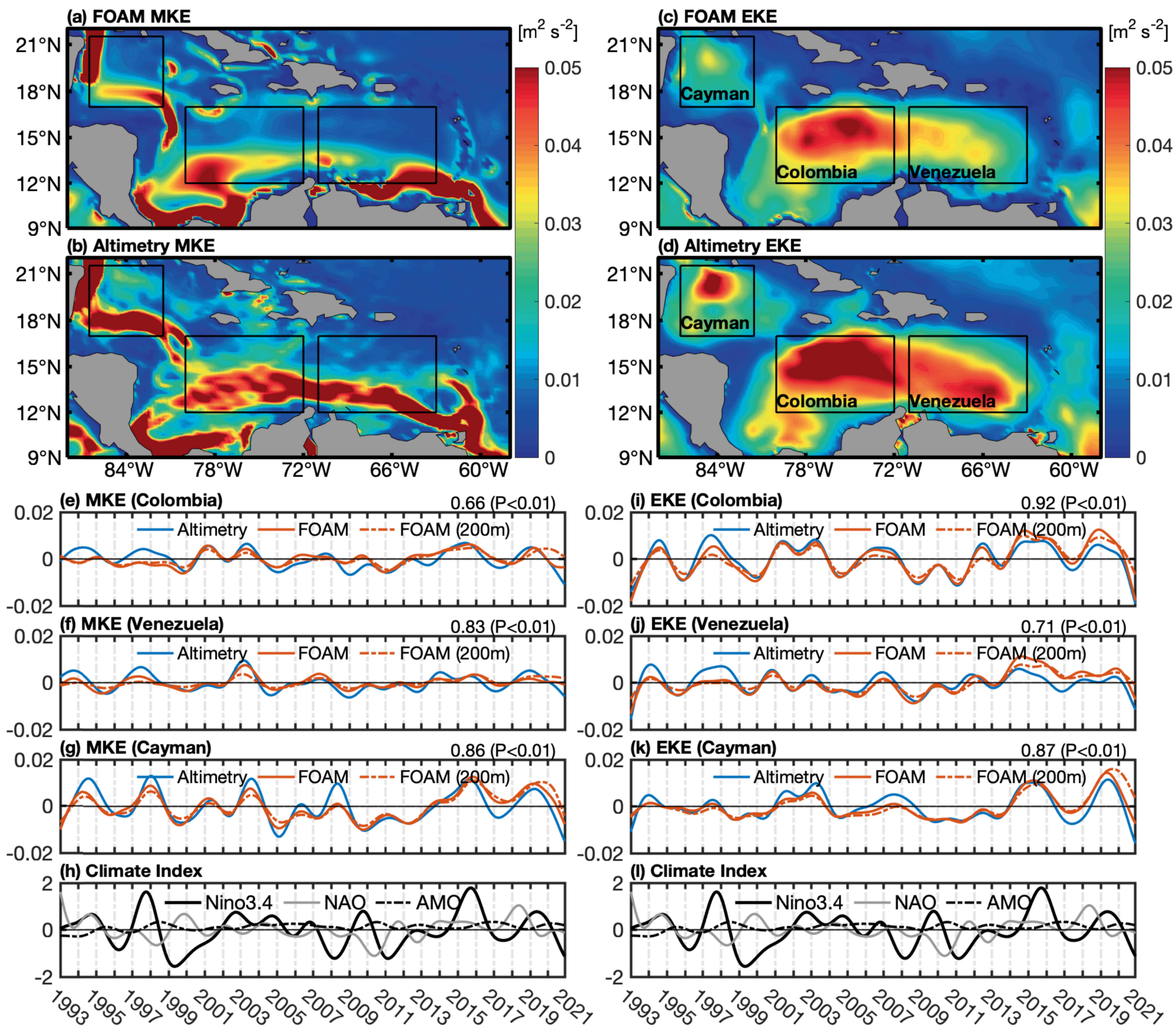

Figure 1. Spatial distribution of the mean (a, b) mean kinetic energy (MKE, m^2 s^{-2}) and (c, d) eddy kinetic energy (EKE, m^2 s^{-2}) from FOAM and altimetry between 1993 and 2020. (e, i), (f, j), (g, k) 2-yr lowpass MKE and EKE (m^2 s^{-2}) anomalies from altimetry and FOAM over the Colombia, Venezuela and Cayman Basin, respectively. Correlation coefficients between altimetry and FOAM as well as the corresponding *p*-values are noted in the top right of each panel. Note that orange dashed lines represent depth-mean (upper 200 m; Figure S2) results from FOAM. The bottom panels (h, l) represent the 2-yr lowpass Niño3.4, NAO, and AMO indices.

Table 1. Correlation coefficients between MKE/EKE and three climate indices in the three basins of the Caribbean Sea. Both results from the altimetry and FOAM are presented. All quoted correlations here are above the 95% significance level except those with underlines.

Correlation coefficient	Altimetry (MKE/EKE)	FOAM (MKE/EKE)	FOAM (200 m) (MKE/EKE)
Colombia & Niño3.4	0.53/0.59	0.52/0.58	0.47/0.57
Venezuela & Niño3.4	0.48/0.36	0.44/0.41	0.49/0.41
Cayman & Niño3.4	0.46/0.50	0.51/0.54	0.50/0.53
Colombia & NAO	0.21/0.06	0.05/0.13	0.09/0.22
Venezuela & NAO	0.21/0.004	0.05/0.22	0.18/0.29
Cayman & NAO	0.15/0.12	0.20/0.23	0.22/0.29
Colombia & AMO	-0.32/-0.04	0.07/0.09	0.08/0.07
Venezuela & AMO	-0.31/-0.20	0.01/0.03	0.10/0.04
Cayman & AMO	-0.15/-0.19	0.001/-0.04	0.07/-0.015

Besides ENSO, we also examine correlations between NAO, AMO and MKE/EKE in the Caribbean Sea. The results (Table 1) show that their relationships are not as substantial as ENSO, and in many cases not even statistically significant. For instance, the altimetry MKE in the Colombia Basin shows much lower correlation coefficients, with ~0.2 for NAO and ~-0.3 for AMO, but the corresponding FOAM MKE in the Colombia Basin is not significantly correlated with either NAO or AMO. For EKE, the relationships with NAO and AMO are even less clear. So, NAO and AMO likely play minor or no roles in modulating the MKE and EKE in the Caribbean Sea, and we will focus on the effects of ENSO in the rest of this paper.

We then investigate how mean currents and eddies in the Caribbean Sea are modulated by ENSO. Firstly, we look at the mean states of the Caribbean Sea. Figure 2a shows that an intense and persistent easterly wind exists in the Caribbean Sea (Wang, 2007). This wind directly controls the intensity and occurrence of the upwelling in the southern Caribbean Sea (Montoya-Sánchez et al., 2018), which appears as a cold SST patch in Figure 2b. The easterly wind also drives the water to pile up in the northern Caribbean Sea through Ekman transport and contributes to the SSH difference between the north and south Caribbean Sea. And the mean currents in the Caribbean Sea are largely determined by the horizontal gradients of the SSH (Figure 2c).

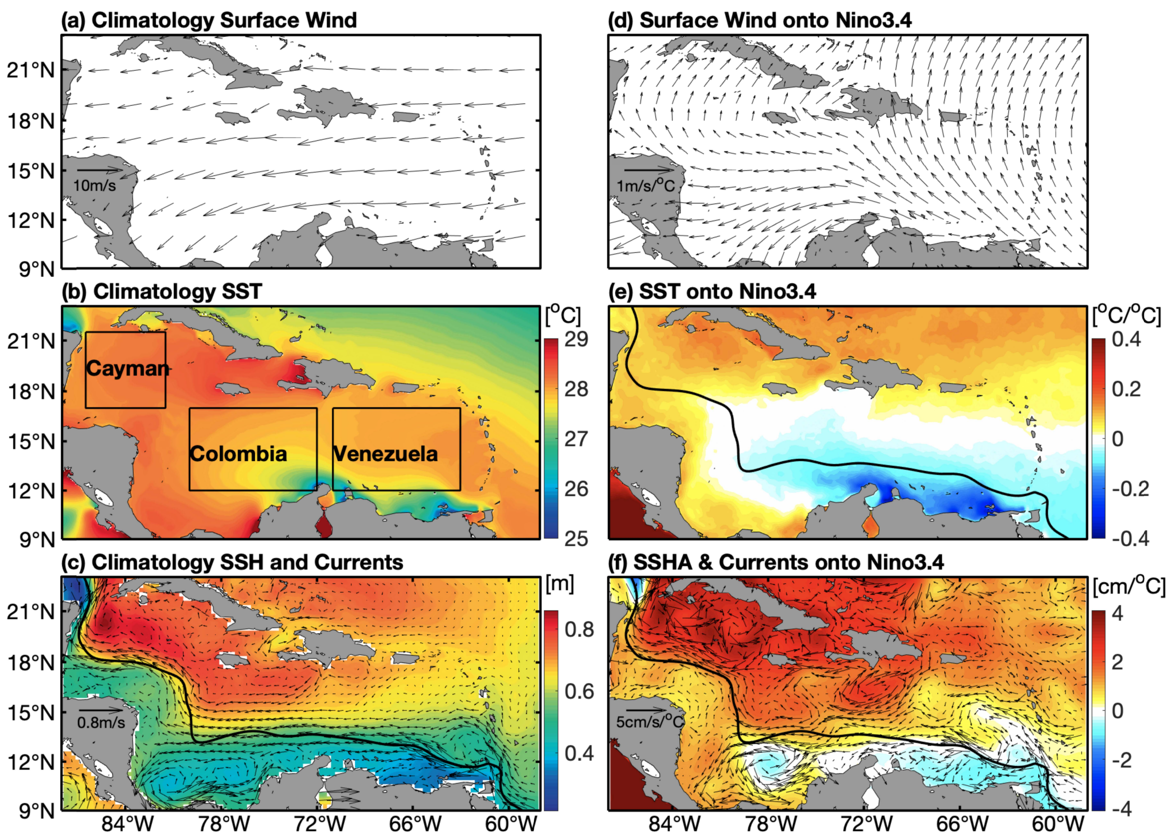

Figure 2. Climatology of (a) surface wind velocity, (b) sea surface temperature (SST), and (c) SSH and geostrophic currents. Spatial distribution of linear regression coefficients of (d) Wind (e) SST, and (f) SSHA and currents onto the Niño3.4 index. The black solid line in (c) represents the maximum speed of the climatology mean current and is also shown in (e) and (f).

We then regress the wind velocity, SST, and sea surface height anomalies (SSHA) onto the Niño3.4 index (Figure 2d-f). The regression analysis shows that positive Niño3.4 indices (El Niño) are associated with an anticyclonic wind anomaly in the Caribbean Sea (Figure 2d). This wind pattern will drive an oceanic convergence and hence higher sea levels in the northern

Caribbean Sea. In the meantime, the easterly wind anomalies in the southern Caribbean Sea can intensify the regional upwelling (Figure 2e). As a consequence, the north-south SSH differences in the Caribbean Sea will increase and strengthen the mean currents though geostrophic balance during El Niño events (Figure 2f). During La Niña events, on the contrary, westerly wind anomalies occur, the upwelling in the southern Caribbean Sea is suppressed (Sayol et al., 2022), SSH north-south differences decreases, and the mean currents in the Caribbean Sea are weakened. This process is also confirmed with the significant correlations between the Niño3.4 index and MKE in the three Caribbean basins (Table 1).

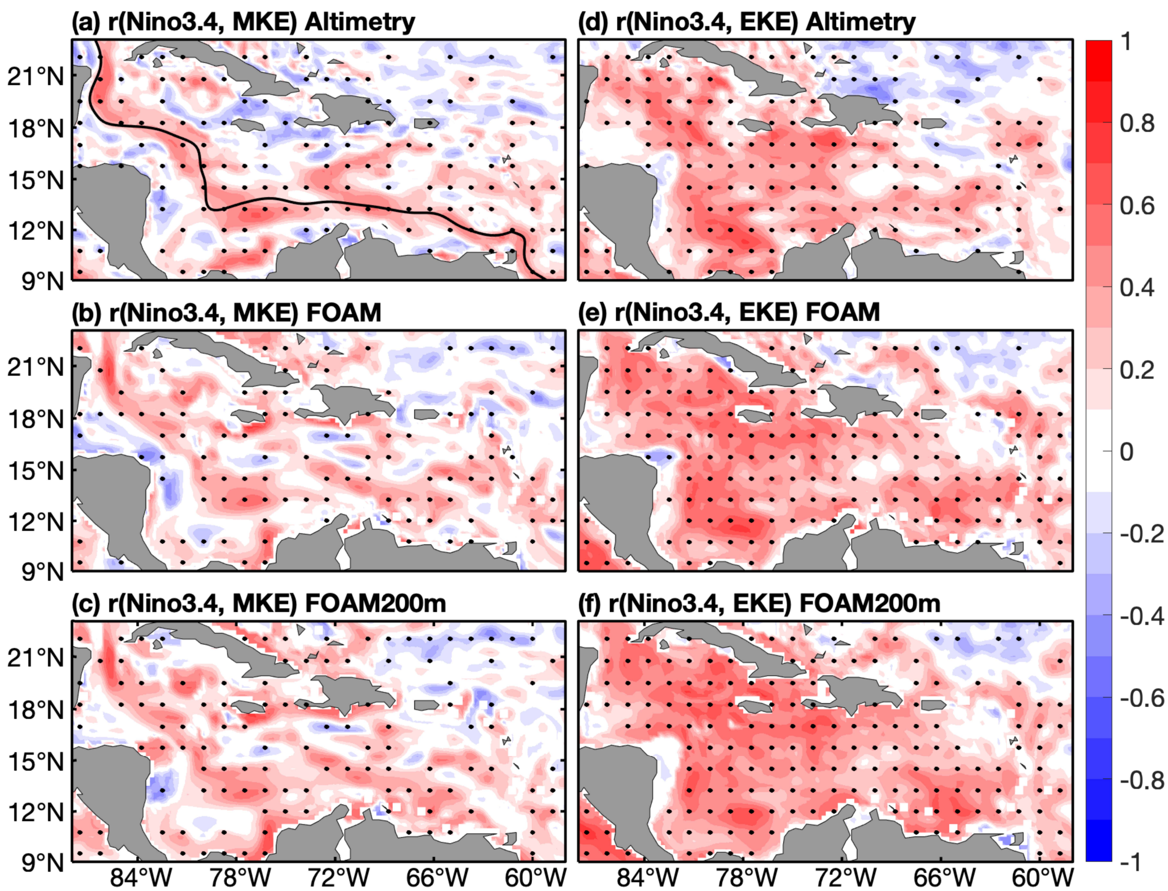

Figure 3. (Left) Correlation coefficients between MKE and Niño3.4 index from (a) altimetry, (b) FOAM, (c) depth-mean (200 m) FOAM. (Right) Same as (left), but for EKE. The black line in (a) represents the maximum speed of the climatology mean current. Correlations above the 95% significance level are marked as black dots.

Correlation coefficients between the Niño3.4 index and MKE/EKE from altimetry and FOAM are also directly calculated and displayed in Figure 3. Significant high correlations between the Niño3.4 index and MKE/EKE over the Caribbean Sea are shown in both products. For the MKE, the highest correlations are primarily confined along the position of the mean current (Figure 3a-c). As suggested above, the synchronized MKE evolution with ENSO in the whole Caribbean Sea is established through ENSO's impacts on the north-south SSH differences and hence the geostrophic currents. Like the MKE, the EKE in the Caribbean Sea also exhibits synchronized variability with the Niño3.4 index but their responses are not confined along the mean current but cover a much larger area (Figure 3d-f).

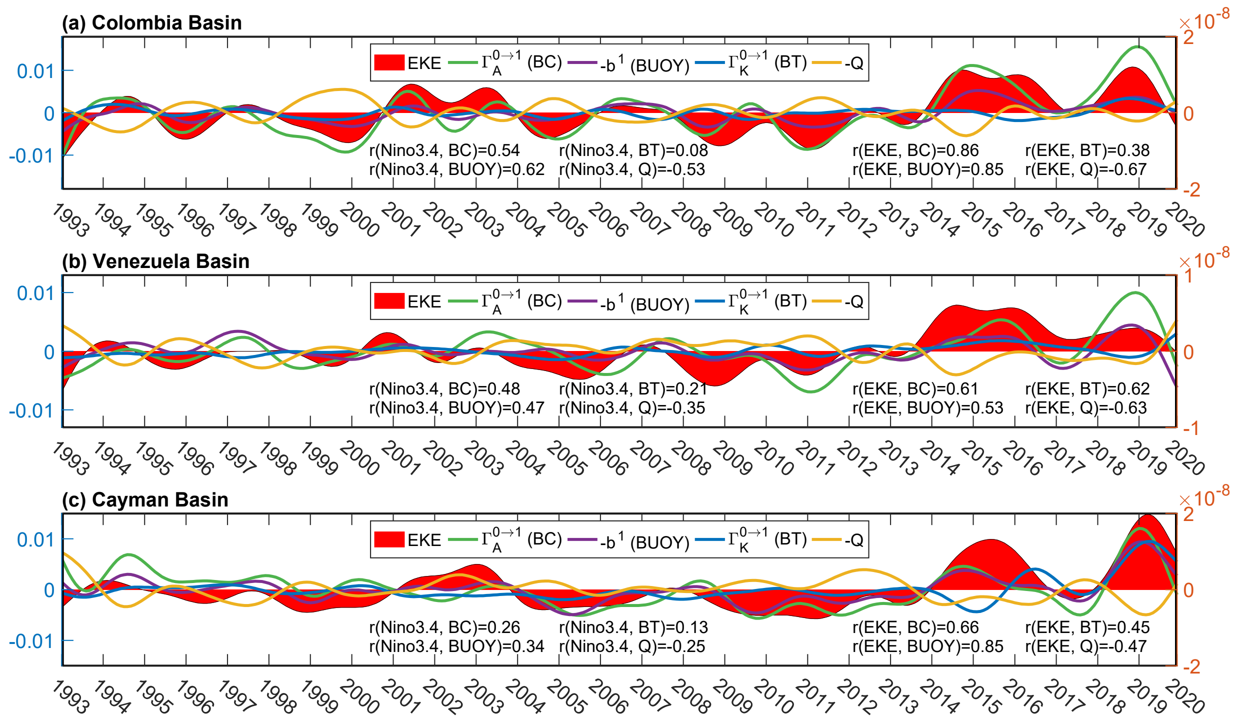

Figure 4. (a) Time series of the area-mean and depth-mean (upper 200 m) EKE and four dynamic processes over the Colombia Basin from FOAM. The terms are baroclinic transfer (BC, green), buoyancy conversion (buoy, purple), barotropic transfer (BT, blue), and nonlocal process (Q, yellow). All the time series are 2-yr low-pass filtered. The units of the EKE budget terms and EKE are m^2 s^{-3} and m^2 s^{-2}, respectively. (b, c) As in (a), but for the Venezuela Basin and Cayman Basin, respectively. The correlation coefficients, r, between four dynamic processes, EKE and the Niño3.4 index are shown in the bottom of each panel.

We then explore the underlying mechanisms for the effects of ENSO on the interannual variability of EKE in the Caribbean Sea. Temporal evolutions of EKE and the related dynamic processes, which were obtained using the MWT-based localized multiscale energy analysis (Liang, 2016), over the three Caribbean basins are displayed in Figure 4. The high correlation between baroclinic transfer (BC, $\Gamma_A^{0\to1}$), buoyancy conversion (b^1) and EKE indicate that baroclinic instability dominates the EKE variability. The barotropic transfer (BT, $\Gamma_k^{0\to1}$) also exhibits positive correlation with the EKE, but its magnitude is much smaller than the BC term (Figure S3). The nonlocal term (combined effect of advection and pressure work) is negatively correlated with the EKE, suggesting that the EKE generated through the instability processes is damped by nonlocal processes via advection and pressure work.

The correlation coefficients between the Niño3.4 index and each of the four budget terms are also calculated (Figure 4). The baroclinic transfer and buoyancy conversion are more closely related to ENSO than the barotropic term. The nonlocal process is negatively related to Niño3.4. More specifically, in the most energetic Colombia Basin (Figure 4a), the correlation coefficient between the Niño3.4 index and BC is 0.54, but the correlation coefficient between the Niño3.4 index and BT is 0.08, indicating that the effect of ENSO on EKE is mainly through baroclinic instabilities in that basin. In the classical instability formalism, baroclinic instability is proportional to the vertical shear of the horizontal flow (Pedlosky, 1987). We hence check the correlation between the vertical shear of the horizontal flow and the Niño3.4 index, and significant high correlations are found (see Figure S4). This further confirms that ENSO modulates EKE through its effect on the mean currents and energy transfer from the background currents to eddies through baroclinic instabilities.

4. Conclusions and Discussion

In this study, we found substantial and synchronized interannual variabilities of MKE and EKE in the whole Caribbean Sea. These interannual variabilities are also closely related to ENSO, indicating that ENSO can modulate the mean currents and mesoscale eddies in the Caribbean Sea. In addition, although previous studies showed significant dynamic differences between the three basins of the Caribbean Sea (e.g., Jouanno et al., 2008), the synchronized mean currents and eddies responses to ENSO occurs across the whole Caribbean Sea, suggesting that the dynamical separation of the three basins in the Caribbean Sea are timescale dependent.

The modulation of mean currents in the Caribbean Sea by ENSO is established through ENSO's impacts on the north-south SSH differences in the Caribbean Sea, which through geostrophic balance affect the mean currents. During El Niño events, the easterly wind anomalies drive the water to pile up in the northern Caribbean Sea and lower the SSH in the southern Caribbean Sea through Ekman transport. These will lead to increased north-south SSH differences and strengthened the mean current, and during La Niña events the opposite happens. The interannual EKE variability is primarily controlled by baroclinic instability, which releases available potential energy stored in the mean currents to mesoscale eddies. Since the mean currents are modulated by ENSO, high correlations between ENSO and EKE are expected.

Besides ENSO, we also notice weak but, in some cases, significant correlations between MKE/EKE and other climate modes, such as NAO and AMO (Table 1). The altimetry data show that NAO is positively correlated with MKE/EKE, while AMO is negatively correlated. During a 'moderate' El Niño event around 2010, MKE and EKE did not show positive anomalies as expected. On the contrary, MKE and EKE showed negative anomalies. This could be related to the strong negative NAO and weak positive AMO, both of which induced negative MKE/EKE anomalies. In addition, effects of climate modes, such as ENSO, NAO, AMO, the Pacific Decadal Oscillation (PDO), and Pacific/North American Pattern (PNA) on the Caribbean winds have been studied and the Niño3.4 index was found to be the dominant mode (Maldonado et al., 2016). This is consistent with our findings of the leading role of ENSO in modulating mean currents and eddies in the Caribbean Sea.

This study provides an example showing the response of regional seas to ENSO. Our results also suggest some predictability of the mean current and mesoscale eddies in the Caribbean Sea, particularly during strong El Niño and La Niña events. Considering the importance of these currents and eddies in transporting heat, salt, and other biogeochemical materials like chlorophyll, *Sargassum*, and larvae etc., as well as their potential impacts on downstream regions, like the Gulf of Mexico, ENSO's impacts on regional climate and marine ocean ecosystem could be expected and should be investigated in the future.

Acknowledgments

The work was supported in part by National Science Foundation through grant OCE-2122507.

Open Research

All the data used in this study are publicly available. The satellite altimetry (https://doi.org/10.48670/moi-00145) and FOAM (https://doi.org/10.48670/moi-00024) model dataset is from the Copernicus Marine Environment Monitoring Service (CMEMS, https://marine.copernicus.eu/). The sea surface temperature data is from CMEMS (https://doi.org/10.48670/moi-00168). The surface wind from the European Centre for Medium-Range Weather Forecasts (ECMWF) Reanalysis fifth Generation (ERA5) is available at (https://doi.org/10.24381/cds.f17050d7). The NAO (https://www.cpc.ncep.noaa.gov/products/precip/CWlink/pna/nao.shtml) and AMO index (https://psl.noaa.gov/data/correlation/amon.us.long.data) are from National Oceanic and Atmospheric Administration (NOAA). The Niño3.4 index is from Asia-Pacific Data-Research Center is available at (http://apdrc.soest.hawaii.edu/las/v6/dataset?catitem=1261).

Reference

1. Alexander, M. A., Bladé, I., Newman, M., Lanzante, J. R., Lau, N.-C., & Scott, J. D. (2002). The Atmospheric Bridge: The Influence of ENSO Teleconnections on Air–Sea Interaction over the Global Oceans. *Journal of Climate*, *15*(16), 2205–2231. https://doi.org/10.1175/1520-0442(2002)015<2205:TABTIO>2.0.CO;2

2. Alvera-Azcárate, A., Barth, A., & Weisberg, R. H. (2009). The Surface Circulation of the Caribbean Sea and the Gulf of Mexico as Inferred from Satellite Altimetry. *Journal of Physical Oceanography*, *39*(3), 640–657. https://doi.org/10.1175/2008JPO3765.1

3. Andrade, C. A., & Barton, E. D. (2000). Eddy development and motion in the Caribbean Sea. *Journal of Geophysical Research: Oceans*, *105*(C11), 26191–26201. https://doi.org/10.1029/2000JC000300

4. Andrade, C. A., & Barton, E. D. (2005). The Guajira upwelling system. *Continental Shelf Research*, *25*(9), 1003–1022. https://doi.org/10.1016/j.csr.2004.12.012

5. Andrade-Canto, F., Karrasch, D., & Beron-Vera, F. J. (2020). Genesis, evolution, and apocalypse of Loop Current rings. *Physics of Fluids*, *32*(11), 116603. https://doi.org/10.1063/5.0030094

6. Andrade-Canto, F., Beron-Vera, F. J., Goni, G. J., Karrasch, D., Olascoaga, M. J., & Triñanes, J. (2022). Carriers of *Sargassum* and mechanism for coastal inundation in the Caribbean Sea. *Physics of Fluids*, *34*(1), 016602. https://doi.org/10.1063/5.0079055

7. Astor, Y., Muller-Karger, F., & Scranton, M. I. (2003). Seasonal and interannual variation in the hydrography of the Cariaco Basin: implications for basin ventilation. *Continental Shelf Research*, *23*(1), 125–144. https://doi.org/10.1016/S0278-4343(02)00130-9

8. Blockley, E. W., Martin, M. J., McLaren, A. J., Ryan, A. G., Waters, J., Lea, D. J., et al. (2014). Recent development of the Met Office operational ocean forecasting system: an overview and assessment of the new Global FOAM forecasts. *Geoscientific Model Development*, *7*(6), 2613–2638. https://doi.org/10.5194/gmd-7-2613-2014

9. Carton, J. A., & Chao, Y. (1999). Caribbean Sea eddies inferred from TOPEX/POSEIDON altimetry and a 1/6° Atlantic Ocean model simulation. *Journal of Geophysical Research: Oceans*, *104*(C4), 7743–7752. https://doi.org/10.1029/1998JC900081

10. Chang, Y.-L., & Oey, L.-Y. (2013). Coupled Response of the Trade Wind, SST Gradient, and SST in the Caribbean Sea, and the Potential Impact on Loop Current's Interannual Variability*. *Journal of Physical Oceanography*, *43*(7), 1325–1344. https://doi.org/10.1175/JPO-D-12-0183.1

11. Chérubin, L. M., & Richardson, P. L. (2007). Caribbean current variability and the influence of the Amazon and Orinoco freshwater plumes. *Deep Sea Research Part I: Oceanographic Research Papers*, *54*(9), 1451–1473. https://doi.org/10.1016/j.dsr.2007.04.021

12. Dong, S., Volkov, D. L., Goni, G., Pujiana, K., Tagklis, F., & Baringer, M. (2022). Remote Impact of the Equatorial Pacific on Florida Current Transport. *Geophysical Research Letters*, *49*(4). https://doi.org/10.1029/2021GL096944

13. Enfield, D. B., & Mayer, D. A. (1997). Tropical Atlantic sea surface temperature variability and its relation to El Niño-Southern Oscillation. *Journal of Geophysical Research: Oceans*, *102*(C1), 929–945. https://doi.org/10.1029/96JC03296

14. Giannini, A., Cane, M. A., & Kushnir, Y. (2001). Interdecadal Changes in the ENSO Teleconnection to the Caribbean Region and the North Atlantic Oscillation*. *Journal of Climate*, *14*(13), 2867–2879. https://doi.org/10.1175/1520-0442(2001)014<2867:ICITET>2.0.CO;2

15. Good, S., Fiedler, E., Mao, C., Martin, M. J., Maycock, A., Reid, R., et al. (2020). The Current Configuration of the OSTIA System for Operational Production of Foundation Sea Surface Temperature and Ice Concentration Analyses. *Remote Sensing*, *12*(4), 720. https://doi.org/10.3390/rs12040720

16. Gordon, A. L. (1967). Circulation of the Caribbean Sea. *Journal of Geophysical Research*, *72*(24), 6207–6223. https://doi.org/10.1029/JZ072i024p06207

17. Hersbach, H., Bell, B., Berrisford, P., Hirahara, S., Horányi, A., Muñoz-Sabater, J., et al. (2020). The ERA5 global reanalysis. *Quarterly Journal of the Royal Meteorological Society*, *146*(730), 1999–2049. https://doi.org/10.1002/qj.3803

18. Huang, M., Liang, X., Zhu, Y., Liu, Y., & Weisberg, R. H. (2021). Eddies Connect the Tropical Atlantic Ocean and the Gulf of Mexico. *Geophysical Research Letters*, *48*(4). https://doi.org/10.1029/2020GL091277

19. Huang, M., Yang, Y., & Liang, X. (2023). Seasonal Eddy Variability in the Northwestern Tropical Atlantic Ocean. *Journal of Physical Oceanography*. https://doi.org/10.1175/JPO-D-22-0200.1

20. Johns, E. M., Muhling, B. A., Perez, R. C., Müller-Karger, F. E., Melo, N., Smith, R. H., et al. (2014). Amazon River water in the northeastern Caribbean Sea and its effect on larval reef fish assemblages during April 2009. *Fisheries Oceanography*, *23*(6), 472–494. https://doi.org/10.1111/fog.12082

21. Johns, W. E., Townsend, T. L., Fratantoni, D. M., & Wilson, W. D. (2002). On the Atlantic inflow to the Caribbean Sea. *Deep Sea Research Part I: Oceanographic Research Papers*, *49*(2), 211–243. https://doi.org/10.1016/S0967-0637(01)00041-3

22. Jouanno, J., & Sheinbaum, J. (2013). Heat Balance and Eddies in the Caribbean Upwelling System. *Journal of Physical Oceanography*, *43*(5), 1004–1014. https://doi.org/10.1175/JPO-D-12-0140.1

23. Jouanno, J., Sheinbaum, J., Barnier, B., Molines, J.-M., Debreu, L., & Lemarié, F. (2008). The mesoscale variability in the Caribbean Sea. Part I: Simulations and characteristics with an embedded model. *Ocean Modelling*, *23*(3–4), 82–101. https://doi.org/10.1016/j.ocemod.2008.04.002

24. Jouanno, J., Sheinbaum, J., Barnier, B., & Molines, J.-M. (2009). The mesoscale variability in the Caribbean Sea. Part II: Energy sources. *Ocean Modelling*, *26*(3–4), 226–239. https://doi.org/10.1016/j.ocemod.2008.10.006

25. Jouanno, J., Sheinbaum, J., Barnier, B., Molines, J. M., & Candela, J. (2012). Seasonal and Interannual Modulation of the Eddy Kinetic Energy in the Caribbean Sea. *Journal of Physical Oceanography*, *42*(11), 2041–2055. https://doi.org/10.1175/JPO-D-12-048.1

26. Laxenaire, R., Chassignet, E. P., Dukhovskoy, D. S., & Morey, S. L. (2023). Impact of upstream variability on the Loop Current dynamics in numerical simulations of the Gulf of Mexico. Frontiers in Marine Science, 10, 1080779. https://doi.org/10.3389/fmars.2023.1080779

27. Liang, X. S., & Anderson, D. G. M. (2007). Multiscale Window Transform. *Multiscale Modeling & Simulation*, *6*(2), 437–467. https://doi.org/10.1137/06066895X

28. Liang, X. S. (2016). Canonical Transfer and Multiscale Energetics for Primitive and Quasigeostrophic Atmospheres. *Journal of the Atmospheric Sciences*, *73*(11), 4439–4468. https://doi.org/10.1175/JAS-D-16-0131.1

29. López-Álzate, M. E., Sayol, J.-M., Hernández-Carrasco, I., Osorio, A. F., Mason, E., & Orfila, A. (2022). Mesoscale eddy variability in the Caribbean Sea. *Ocean Dynamics*, *72*(9–10), 679–693. https://doi.org/10.1007/s10236-022-01525-9

30. Maldonado, T., Rutgersson, A., Amador, J., Alfaro, E., & Claremar, B. (2016). Variability of the Caribbean low-level jet during boreal winter: large-scale forcings: CARIBBEAN LOW-LEVEL JET AND ITS VARIABILITY. *International Journal of Climatology*, *36*(4), 1954–1969. https://doi.org/10.1002/joc.4472

31. Malmgren, B. A., Winter, A., & Chen, D. (1998). El Niño–Southern Oscillation and North Atlantic Oscillation Control of Climate in Puerto Rico. *Journal of Climate*, *11*(10), 2713–2717. https://doi.org/10.1175/1520-0442(1998)011<2713:ENOSOA>2.0.CO;2

32. Montoya-Sánchez, R. A., Devis-Morales, A., Bernal, G., & Poveda, G. (2018). Seasonal and intraseasonal variability of active and quiescent upwelling events in the Guajira system, southern Caribbean Sea. *Continental Shelf Research*, *171*, 97–112. https://doi.org/10.1016/j.csr.2018.10.006

33. Muller-Karger, F. E., Astor, Y. M., Benitez-Nelson, C. R., Buck, K. N., Fanning, K. A., Lorenzoni, L., et al. (2019). The Scientific Legacy of the CARIACO Ocean Time-Series Program. *Annual Review of Marine Science*, *11*(1), 413–437. https://doi.org/10.1146/annurev-marine-010318-095150

34. Murphy, S. J., Hurlburt, H. E., & O'Brien, J. J. (1999). The connectivity of eddy variability in the Caribbean Sea, the Gulf of Mexico, and the Atlantic Ocean. *Journal of Geophysical Research: Oceans*, *104*(C1), 1431–1453. https://doi.org/10.1029/1998JC900010

35. Ntaganou, N., Kourafalou, V., Beron-Vera, F. J., Olascoaga, M. J., Le Hénaff, M., & Androulidakis, Y. (2023). Influence of Caribbean eddies on the Loop current system evolution. Frontiers in Marine Science, 10, 961058. https://doi.org/10.3389/fmars.2023.961058

36. Oey, L.-Y. (2004). Vorticity flux through the Yucatan Channel and Loop Current variability in the Gulf of Mexico. *Journal of Geophysical Research*, *109*(C10), C10004. https://doi.org/10.1029/2004JC002400

37. Palanisamy, H., Becker, M., Meyssignac, B., Henry, O., & Cazenave, A. (2012). Regional sea level change and variability in the Caribbean sea since 1950. *Journal of Geodetic Science*, *2*(2), 125–133. https://doi.org/10.2478/v10156-011-0029-4

38. Pedlosky, J., 1987: Geophysical Fluid Dynamics. 2nd ed. Springer-Verlag, 710 pp.

39. Pratt, R. W., & Maul, G. A. (2000). Sea Surface Height Variability of The Intra-Americas Sea From Topex/Poseidon Satellite Altimetry: 1992–1995. *Bulletin Of Marine Science*, *67*(2).

40. Pujol, M.-I., Faugère, Y., Taburet, G., Dupuy, S., Pelloquin, C., Ablain, M., & Picot, N. (2016). DUACS DT2014: the new multi-mission altimeter data set reprocessed over 20years. *Ocean Science*, *12*(5), 1067–1090. https://doi.org/10.5194/os-12-1067-2016

41. Richardson, P. L. (2005). Caribbean Current and eddies as observed by surface drifters. *Deep Sea Research Part II: Topical Studies in Oceanography*, *52*(3–4), 429–463. https://doi.org/10.1016/j.dsr2.2004.11.001

42. Sayol, J., Vásquez, L. M., Valencia, J. L., Linero-Cueto, J. R., García-García, D., Vigo, I., & Orfila, A. (2022). Extension and application of an observation-based local climate index aimed to anticipate the impact of El Niño–Southern Oscillation events on Colombia. *International Journal of Climatology*, *42*(11), 5403–5429. https://doi.org/10.1002/joc.7540

43. Taylor, G. T., Muller-Karger, F. E., Thunell, R. C., Scranton, M. I., Astor, Y., Varela, R., et al. (2012). Ecosystem responses in the southern Caribbean Sea to global climate change. *Proceedings of the National Academy of Sciences*, *109*(47), 19315–19320. https://doi.org/10.1073/pnas.1207514109

44. van der Boog, Jong, M. F., Scheidat, M., Leopold, M. F., Geelhoed, S. C. V., Schulz, K., et al. (2019a). Hydrographic and Biological Survey of a Surface-Intensified Anticyclonic Eddy in the Caribbean Sea. *Journal of Geophysical Research: Oceans*, *124*(8), 6235–6251. https://doi.org/10.1029/2018JC014877

45. van der Boog, Carine G., Pietrzak, J. D., Dijkstra, H. A., Brüggemann, N., van Westen, R. M., James, R. K., et al. (2019b). The impact of upwelling on the intensification of anticyclonic ocean eddies in the Caribbean Sea. *Ocean Science*, *15*(6), 1419–1437. https://doi.org/10.5194/os-15-1419-2019

46. Wang, C. (2007). Variability of the Caribbean Low-Level Jet and its relations to climate. *Climate Dynamics*, *29*(4), 411–422. https://doi.org/10.1007/s00382-007-0243-z

47. Yang, Y., Weisberg, R. H., Liu, Y., & San Liang, X. (2020). Instabilities and Multiscale Interactions Underlying the Loop Current Eddy Shedding in the Gulf of Mexico. *Journal of Physical Oceanography*, *50*(5), 1289–1317. https://doi.org/10.1175/JPO-D-19-0202.1

48. Yeh, S.-W., Cai, W., Min, S.-K., McPhaden, M. J., Dommenget, D., Dewitte, B., et al. (2018). ENSO Atmospheric Teleconnections and Their Response to Greenhouse Gas Forcing. *Reviews of Geophysics*, *56*(1), 185–206. https://doi.org/10.1002/2017RG000568